Journal of Magnetic Resonance 204 (2010) 150–154

Contents lists available at ScienceDirect

Journal of Magnetic Resonance

journal homepage: www.elsevier.com/locate/jmr

Communication

On the magic-angle turning and phase-adjusted spinning sidebands experiments

Ivan Hung, Zhehong Gan *

Center of Interdisciplinary Magnetic Resonance, National High Magnetic Field Laboratory, 1800 East Paul Dirac Drive, Tallahassee, FL 32310, USA

ARTICLE INFO

Article history:
Received 3 November 2009
Revised 25 January 2010
Available online 11 February 2010

Keywords:
MAS
Magic-angle turning
MAT
Phase-adjusted spinning sidebands
PASS
^{13}C
Spinning sidebands
Chemical shift anisotropy
CSA

ABSTRACT

The underlying relation between the magic-angle turning (MAT) and phase-adjusted spinning sidebands (PASS) experiments is examined. The MAT experiment satisfies the PASS conditions for separating spinning sidebands with a non-constant total evolution time and only requires linear t_1 increments of up to one rotor period. The time-domain data of the two experiments are related by a shearing transformation. A combination of the linear evolution-time increments of MAT and simple data processing of PASS are particularly attractive for the implementation of MAT for measuring chemical shift anisotropy.

1. Introduction

Magic-angle spinning (MAS) is an ubiquitous method for high-resolution NMR of solids [1,2]. For dilute spin-1/2 nuclei like ^{13}C and ^{15}N, narrow line widths can be obtained under high-power ^{1}H decoupling even with spinning rates far less than the span of chemical shift anisotropy (CSA). The modulation of CSA by slow sample spinning yields an array of spinning sidebands for every site. The relative intensities of the spinning sideband manifolds contain useful CSA information such as the anisotropy and asymmetry parameters of the CSA tensors [3,4]. At very slow spinning, the spinning sideband profile resembles the static powder patterns which show the frequencies of the three CSA tensor principal components directly. However, the increasing number of spinning sidebands makes the extraction of CSA parameters from multiple atomic sites difficult due to the overlap among the manifolds. This problem can be solved ideally in the form of a two-dimensional experiment [5] that separates the anisotropic patterns in one-dimension by their isotropic chemical shifts along the other dimension. Various methods have been developed along this line by mechanically switching the spinning angle (SAS) [6–8], rapidly changing the spinning state (Stop-and-Go) [9], reconstructing 2D isotropic-CSA spectra from a set of spectra acquired with variable angle spinning axis (VACSY) [10], and numerous CSA recoupling and amplification sequences that reintroduce CSA under fast MAS [11–20].

In the case of slow-to-moderate spinning frequencies, two types of experiments are effective for separating spinning sideband manifolds according to the isotropic chemical shifts. The first method is based on the ingenious TOSS and PASS experiments by Dixon in 1982 [21,22]. Using a small number (typically four or five) of π-pulses, the initial magnetization before the data acquisition can be prepared such that: (1) all spinning sidebands are suppressed except the center band (TOSS), or (2) the spinning sidebands are phase-adjusted according to sideband orders (PASS). The TOSS experiment can yield clean high-resolution spectra without any spinning sidebands, while a combination of PASS spectra with incrementing spinning sideband phase adjustment, or so-called pitch (Θ), is capable of separating spinning sidebands according to sideband order. The Dixon methods have been exploited in various two-dimensional experiments by Kolbert and Griffin [23], DeLacroix et al. [24] and Antzutkin et al. [25]. In comparison, the 2D 5-π PASS experiment by Antzutkin et al. [25] is the most robust with a short constant evolution time equal to one rotor period and straightforward data processing. The 2D-PASS experiment has also been applied to quadrupolar nuclei [26,27]. In this case, nine π-pulses are required for the QPASS experiment because the second-order quadrupolar interaction contains $l = 4$ rank anisotropy as compared to only $l = 2$ rank anisotropy in the case of CSA. Hong and Harbison also introduced the idea of using chemical shift suspension by two phase-inverted pulses for the TOSS/PASS experiments instead of time-evolution reversal using π-pulses [28]. The second approach originates from a non-spinning experiment by Bax et al. [29]. The so-called magic-angle hopping (MAH) experi-

* Corresponding author. Fax: +1 850 644 1366.
E-mail address: gan@magnet.fsu.edu (Z. Gan).

1090-7807/$ - see front matter © 2010 Elsevier Inc. All rights reserved.
doi:10.1016/j.jmr.2010.02.004

ment utilizes the fact that the sum of frequencies at three sample orientations hopped around the magic-angle axis by 120° averages the $l = 2$ rank CSA. High-resolution isotropic spectra can be obtained along the indirect dimension (F_1) by combining three evolution segments of the magic-angle hopping experiment. Later, it was realized that such an averaging still holds true under continuous slow magic-angle spinning, or magic-angle turning (MAT) [30], which is easier to implement using conventional MAS probes than discrete MAH. The π-pulse version of the MAT experiment (5-π MAT) was developed soon after [31] to overcome the factor of 2 signal loss from a pair of π/2-pulses for each projection-storage evolution segment. Because the MAT experiment has high-resolution isotropic spectra along F_1, a large number of t_1 increments is required. This problem can be solved by rearranging the rotational echoes acquired during the t_2 period into the indirect dimension such that t_1 increments up to only one rotor period are needed [32–34]. The MAT experiment has also been applied to quadrupolar nuclei by using five evolution segments that are equally separated by 72° in rotor position [35]. A recent application of MAT to highly disordered samples with large CSA and shift distributions has also been reported [36].

Comparing the 5-π MAT [31] and PASS [25] experiments (Fig. 1), one finds striking similarities but also some differences. Both are constant-time experiments which use five π-pulses within a total evolution time of one rotor period. Their coherence transfer pathways and phase cycling are identical, as are their signal efficiencies. Yet, they differ in the timing of the five π-pulses, data processing and final spectral representation. In this work, we investigate the underlying connection between the two experiments, which have been developed following different paths for the same purpose of separating spinning sideband manifolds. In the original 2D-PASS paper of Antzutkin et al. [25] it was mentioned that the pulse timings of the MAT experiment satisfy the PASS conditions with a non-constant evolution time. The MAT version of PASS was also shown to be less susceptible to weak homonuclear dipolar coupling [37]. We show here that the MAT version of PASS combines some of the advantages from both MAT and PASS, such as the linear evolution-time increments of MAT and the straightforward data processing of PASS.

2. Theory

The principle behind MAT is that the sum of three evolution segments 120° rotor positions apart averages $l = 2$ rank anisotropy [29,30]; the theory for the experiment can be described without the need for equations. There are a total of six evolution segments for the 5-π MAT pulse sequence as depicted in Fig. 1. The selected coherence transfer pathway alternates between the $p = +1$ and -1 inverted five times by the π-pulses resulting in the + and − signs in Fig. 1b for each evolution segment. In the pulse timing diagrams, the second and fourth π-pulses are fixed at 1/3 and 2/3 of the rotor period (τ_r), while the other three pulses move together and pass through $\tau_r/6$, $3\tau_r/6$ and $5\tau_r/6$ at $t_1 = 0$ in a manner similar to constant-time experiments (Fig. 1b). Such a timing keeps each of the three $p = +1$ and -1 evolution segments 120° apart in terms of rotor position, satisfying the magic-angle hopping/turning condition. The net evolution of the anisotropic chemical shift is therefore kept equal to zero for all t_1 increments. The isotropic part of the chemical shift (ω_{iso}) is not modulated by the sample rotation and evolves simply as $\omega_{iso}t_1$ because the difference in total duration between the $p = +1$ and -1 evolution periods is equal to t_1. During t_2 acquisition, modulation of the CSA

$$\omega(t) = \sum_{m=\pm l}^{\pm l} \omega_m \exp(im\omega_r t) \tag{1}$$

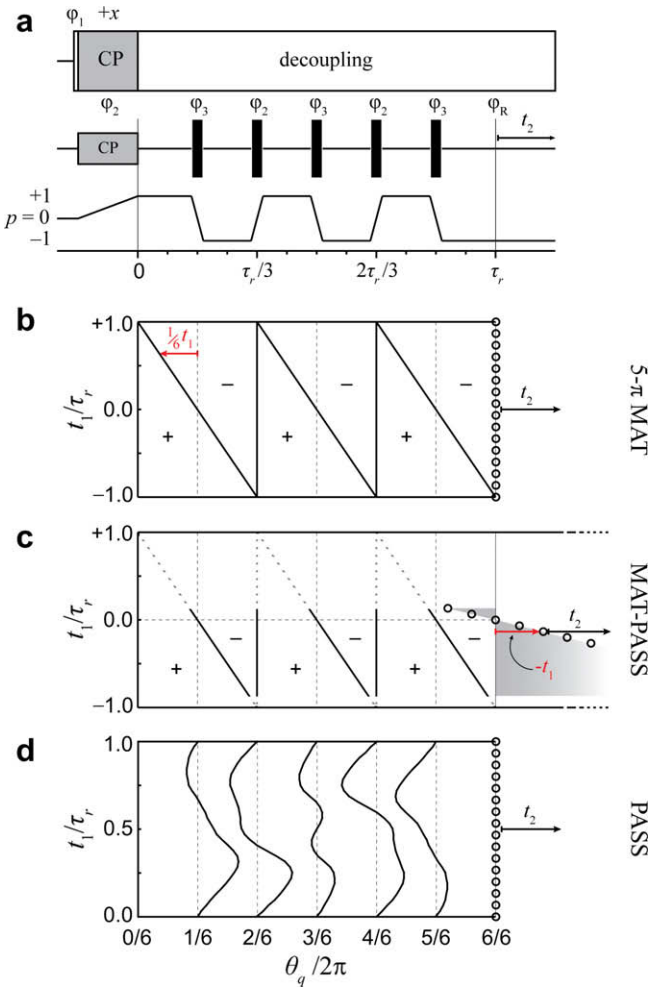

Fig. 1. (a) Pulse sequence and timings θ_q as fractions of one rotor period for (b) 5-π MAT, (c) MAT version of PASS and (d) PASS pulse sequences. A 12-step cogwheel phase cycling scheme [38] determined using the program described in Ref. [39] selects the desired coherence transfer pathway: $\varphi_1 = \pi/2$, $\varphi_2 = 0$, $\varphi_3 = \{0, 1, 2, 3, 4, 5, 6, 7, 8, 9, 10, 11\} \times 2\pi/12$ and $\varphi_R = \{0, \pi\}$. Additional phase inversion of φ_1 and φ_R eliminates artifacts due to DC offset. Solid black bars in the pulse sequence denote π-pulses. Circles denote the beginning of t_2 acquisition, while positive and negative signs denote the sign of the evolving coherence order. Note that the t_1 increments span exactly one rotor period and the beginning of t_2 acquisition is shifted by $-t_1$ (shaded area) for MAT–PASS as compared to the original MAT experiment to obtain PASS spectra.

by MAS yields spinning sidebands along F_2

$$\left\langle \exp\left(-i\int_{t_1}^{t_2} \omega(t)dt\right)\right\rangle = \sum_k s_k \exp(ik\omega_r t_2) \tag{2}$$

where $\langle\rangle$ denotes powder averaging and s_k are the intensities of the spinning sideband manifold. The 2D time-domain signal of the MAT experiment can thus be expressed as

$$S^{MAT}(t_1, t_2) = \sum_k s_k \exp(-i\omega_{iso}t_1)\exp(-i\omega_{iso}t_2 + ik\omega_r t_2) \tag{3}$$

The two exponentials represent the t_1 (isotropic), and t_2 (isotropic and anisotropic) chemical shift modulations. Fig. 1 shows a total evolution time of one rotor period, which is sufficient for the PASS-type experiments. Longer t_1 values for regular MAT experiments can be obtained by extending the total evolution time to any integer number of rotor periods other than multiples of 3. In the case of quadrupolar nuclei, two groups ($p = \pm 1$) of five evolution segments using nine π-pulses are required to average aniso-

tropic broadening of ranks up to $l = 4$ [35]. The segments are 72° apart in rotor position and the total evolution time can be any integer number of rotor periods other than multiples of 5.

The theory behind PASS is more intriguing and can be found in the original Dixon paper [22] as well as the 2D-PASS paper by Antzutkin et al. [25]. A condensed version for general 2D-PASS experiments using n π-pulses is presented here for comparison with MAT. The timing of the π-pulses of PASS experiments satisfies two conditions. The first condition ensures no isotropic shift evolution by making the total durations of the p = +1 and −1 evolution segments equal

$$\sum_{q=0}^{n}(-1)^{n+q}(\theta_{q+1}-\theta_q)=0 \tag{4}$$

We use rotation angles $\theta_q = \omega_r t_q$ (q = 1 to n) to describe the timing of the π-pulses, where θ_0 and θ_{n+1} denote the beginning and end of the t_1-evolution period. The second condition makes the net evolution of the MAS-modulated anisotropic shift $\omega(t)$ for the PASS period equivalent to a continuous t_1 evolution prior to the start of t_2 acquisition,

$$\sum_{q=0}^{n}\left[(-1)^{n+q}\int_{\theta_q/\omega_r}^{\theta_{q+1}/\omega_r}\omega(t)dt\right]=\int_{\theta_{n+1}/\omega_r-t_1}^{\theta_{n+1}/\omega_r}\omega(t)dt \tag{5}$$

We use evolution time t_1 instead of pitch Θ (Ref. [25]) for ease of comparison with the MAT experiment; the two variables are related by $\Theta = -\omega_r t_1$. The second condition leads to a set of non-linear equations when the coefficients of ω_m are equated after insertion of Eq. (1) into Eq. (5),

$$\sum_{q=0}^{n}(-1)^{n+q}[\exp(im\theta_{q+1})-\exp(im\theta_q)] = \exp(im\theta_{n+1})-\exp[im(\theta_{n+1}-\omega_r t_1)] \tag{6}$$

Solution of the so-called PASS equations (Eqs. (4) and (6)) determines the timing of π-pulses for PASS experiments [25]. The timings for isolation of the $l = 2$ rank CSA in F_1 using five π-pulses and a constant evolution time of one rotor period ($\theta_0 = 0$ and $\theta_{n+1} = 2\pi$) are shown in Fig. 1d. The two conditions for PASS experiments lead to the following time-domain signal after powder averaging

$$\begin{aligned}S^{\mathrm{PASS}}(t_1,t_2) &= \left\langle \exp\left(-i\int_{\theta_{n+1}/\omega_r-t_1}^{\theta_{n+1}/\omega_r}\omega(t)dt\right)\exp\left(-i\int_{\theta_{n+1}/\omega_r}^{\theta_{n+1}/\omega_r+t_2}\omega(t)dt\right)\right.\\ &\quad\left.\times\exp(-i\omega_{iso}t_2)\right\rangle\\ &= \left\langle \exp\left(-i\int_{\theta_{n+1}/\omega_r-t_1}^{\theta_{n+1}/\omega_r+t_2}\omega(t)dt\right)\exp(-i\omega_{iso}t_2)\right\rangle\\ &= \sum_k s_k\exp(ik\omega_r t_1)\exp(-i\omega_{iso}t_1+ik\omega_r t_2)\end{aligned} \tag{7}$$

The two exponentials represent the t_1 (anisotropic), and t_2 (isotropic and anisotropic) chemical shift modulations. 2D Fourier transformation of the PASS signal separates the spinning sidebands by their order k for linear t_1 increments spanning integer rotor periods. Comparison of Eqs. (3) and (7) reveals only a difference in the selection of either the isotropic or anisotropic chemical shifts

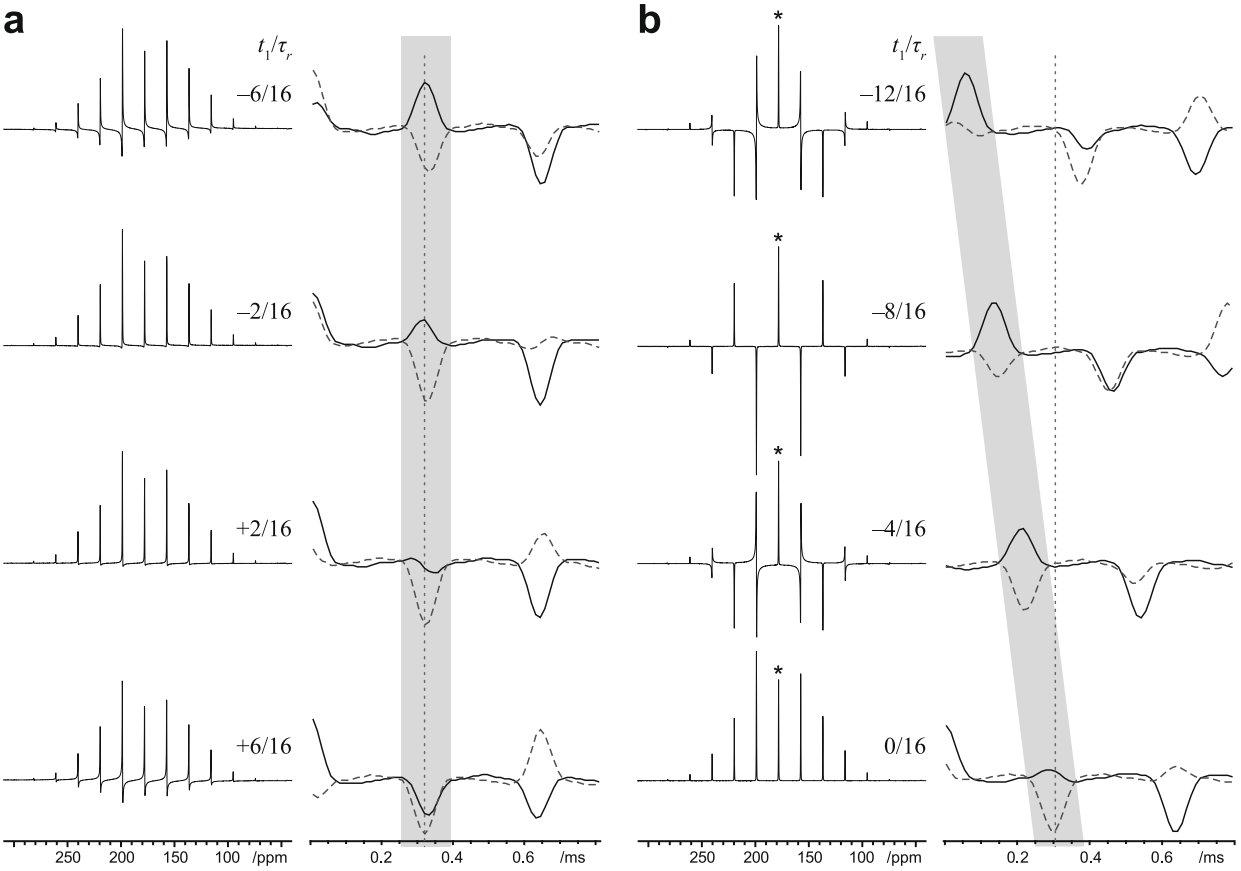

Fig. 2. Select t_1 slices along F_2 and time-domain signals of (a) 5-π MAT and (b) MAT–PASS spectra for [^{13}C′]glycine acquired at B_0 = 14.1 T and 3125 Hz MAS. The first three rotational echoes of the time-domain signals are plotted. The real and imaginary components of the time-domain signals are shown as solid and dashed lines, respectively. The dotted vertical lines denote the timing of the first rotor period. Gray bars highlight the stationary and travelling echoes of the MAT and MAT–PASS signals, respectively. Asterisk (*) denotes the isotropic center band.

in t_1 by MAT and PASS, respectively. The time-domain signals of the two experiments can be related through a shift of the t_2 acquisition by a time $-t_1$ (i.e., $t_2 \rightarrow t_2 - t_1$),

$$S^{\mathrm{PASS}}(t_1, t_2) = S^{\mathrm{MAT}}(t_1, t_2 - t_1) \tag{8}$$

This is the central result relating the MAT and PASS experiments.

Fig. 1c shows the timing of π-pulses and t_2 acquisition for the MAT version of PASS. The evolution time t_1 spans one rotor period as required by the 2D processing (using Fourier transformations) of PASS-type spectra. The start of t_2 acquisition cannot precede the last π-pulse, therefore most of the evolution increments are in negative t_1 (grey highlighted area in Fig. 1c). The experimental implementation can be described by the delays τ_i before the ith pulse: $\tau_1 = \tau_3 = \tau_5 = [2 - (n+x)/N]\tau_r/6$, $\tau_2 = \tau_4 = [(n+x)/N]\tau_r/6$, and the delay before t_2 acquisition $\tau_6 = [6 - 5(n+x)/N]\tau_r/6$, where τ_r is the rotor period, n is the t_1-slice counter beginning from 1, N is the total number of increments, and x is a small positive integer (usually 2) which shifts the t_1 range to avoid timing conflicts. The pulse lengths also need to be considered in the delays. This MAT experiment has a non-constant evolution time as shown in Fig. 1 in contrast to the constant-time 5-π PASS experiment.

3. Results and discussion

Fig. 2 shows a comparison of spectra and time-domain signals between MAT and MAT–PASS for various t_1 increments. The MAT signal is phase-modulated in t_1 by the isotropic chemical shift as seen from the change of peak phases and the relative intensities between the real and imaginary components of the signal. The phase change is gradual due to the proximity of the center band to the carrier frequency. Notably, the rotational echoes remain stationary as t_1 progresses. In contrast, PASS-type spectra show no modulation to the center band in accordance with the null isotropic shift evolution in t_1, while sidebands are phase-modulated according to their orders. In the time-domain, the first-order phasing manifests itself as a shift of the rotational echoes, as highlighted by the travelling echoes in Fig. 2b as t_1 progresses.

The separation of spinning sideband manifolds by MAT–PASS is demonstrated using a L-histidine sample lyophilized at pH 1.7 (Fig. 3a). The 1D CP/MAS spectrum at a low spinning rate is crowded with spinning sidebands. The center-band-only spectrum at $F_1 = 0$ of the 2D MAT–PASS spectrum reveals the number of distinct carbon sites directly, while a sum of the slices allows reconstruction of the CP/MAS spectrum. The number of distinct resonances is higher than expected due to the presence of two polymorphs [40]. The other F_1 slices shows separated spinning sidebands with their intensities containing the CSA information. The efficiency and residual intensity of separated sidebands are similar to that of the conventional PASS experiment (not shown). Fig. 3b shows a representation of the 2D MAT–PASS spectrum after a shear transformation along the F_2 axis such that spinning sidebands become aligned along F_1. The sheared spectrum gives the isotropic chemical shift along F_2 and spinning sideband order along F_1. A sum projection along F_2 yields an 'infinite speed' MAS spectrum that is quantitative and free of spinning sidebands.

The MAT–PASS experiment is one of many possible experiments which satisfy the PASS equations [25,37]. The conventional implementation of PASS [25] opts for a solution with a constant evolution time to avoid the adverse effects of relaxation. However, the typical solution of the non-linear PASS equations does not result in the linear variation of pulse timings commonly employed in 2D experiments. In contrast, MAT–PASS provides a non-constant-time PASS solution that results in linearly incrementing pulse delays. The linear increment is of particular advantage/convenience for practical implementation of MAT–PASS. The number of t_1 increments can be set to arbitrary values as with conventional 2D experiments without the need for entering numerous delays from pre-solving the non-linear PASS equations. On the other hand,

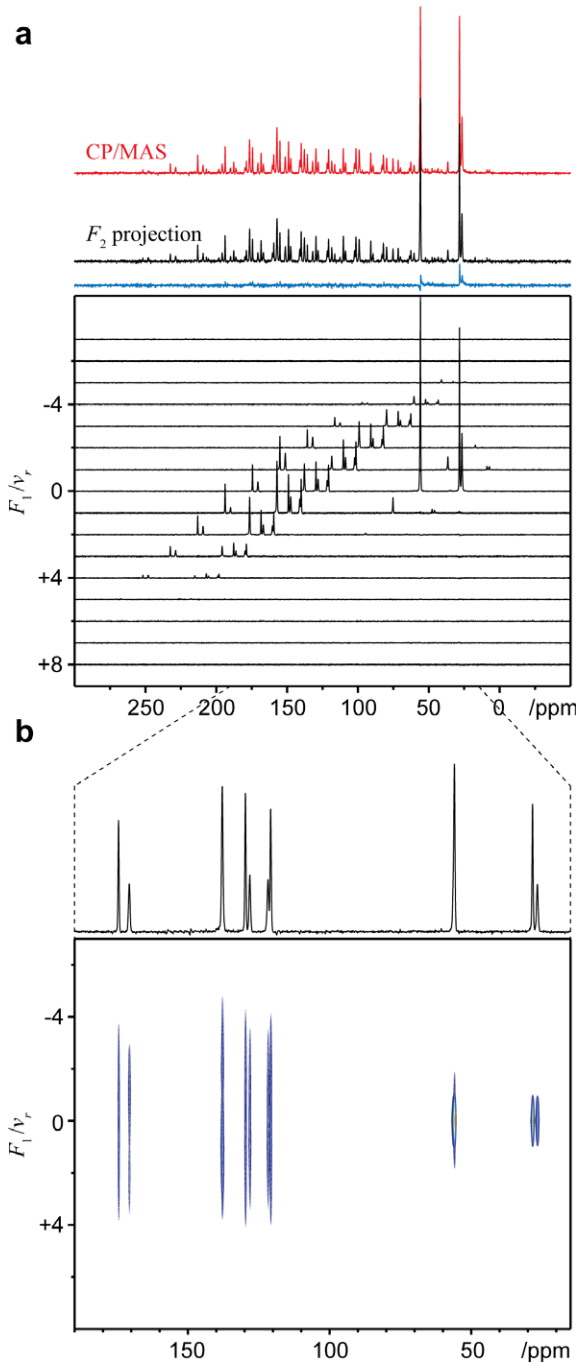

Fig. 3. (a) ^{13}C CP/MAS (shown in red) and MAT–PASS spectra of L-histidine (pH 1.7) acquired at $B_0 = 14.1$ T and 2920 Hz MAS. The difference between the CP/MAS spectrum and the projection along F_2 is shown in blue. (b) 2D spectrum obtained after shearing of (a) to align spinning sidebands along F_1 with summed projection shown on top. The number of resonances is higher than expected due to the presence of two polymorphs [35]. Experiments were performed on a Bruker Avance 600 spectrometer using a 4 mm MAS probe. The rf field are 71.4 and 100 kHz, respectively, for ^{13}C π-pulses and ^{1}H heteronuclear decoupling. A total of 16 increments over a t_1 range of $[-7\tau_r/8, +\tau_r/8]$ were employed to avoid overlap between t_2-acquisition and the last π-pulse. Spectral phasing on F_2 was performed on the $t_1 = 0$ slice, while a first-order phase of $(n_{t_1=0} - 1) \cdot 360^\circ$ was applied on the F_1, where $n_{t_1=0}$ is the slice number for the $t_1 = 0$ slice. (For interpretation of the references to color in this figure legend, the reader is referred to the web version of this paper.)

MAT–PASS spectra are subjected to relaxation effects due to the non-constant evolution time. The MAT–PASS evolution time spans no more than one rotor period, thus the adverse effects of relaxation are expected to be small if efficient proton decoupling is employed and the rotor period is short compared to transverse relaxation, as exemplified with L-histidine (pH 1.7).

4. Conclusion

The 2D MAT and PASS experiments isolate the isotropic and anisotropic chemical shifts in the indirect dimension, respectively. It has been shown both theoretically and experimentally that these two experiments are related by shifting the t_2-acquisition. The MAT–PASS experiment yields PASS-like spectra using linear t_1 increments and is easy to implement for the separation of spinning sidebands.

Acknowledgments

This work was supported by the National High Magnetic Field Laboratory through National Science Foundation Cooperative Agreement (DMR-0084173) and by the State of Florida.

References

[1] E.R. Andrew, A. Bradbury, R.G. Eades, Removal of dipolar broadening of nuclear magnetic resonance spectra of solids by specimen rotation, Nature (London UK) 183 (1959) 1802–1803.
[2] J. Schaefer, E.O. Stejskal, Carbon-13 nuclear magnetic resonance of polymers spinning at the magic angle, J. Am. Chem. Soc. 98 (1976) 1031–1032.
[3] M.M. Maricq, J.S. Waugh, NMR in rotating solids, J. Chem. Phys. 70 (1979) 3300–3316.
[4] J. Herzfeld, A.E. Berger, Sideband intensities in NMR-spectra of samples spinning at the magic angle, J. Chem. Phys. 73 (1980) 6021–6030.
[5] W.P. Aue, E. Bartholdi, R.R. Ernst, 2-Dimensional spectroscopy – application to nuclear magnetic-resonance, J. Chem. Phys. 64 (1976) 2229–2246.
[6] A. Bax, N.M. Szeverenyi, G.E. Maciel, Chemical-shift anisotropy in powdered solids studied by 2D FT CP MAS NMR, J. Magn. Reson. 51 (1983) 400–408.
[7] T. Terao, T. Fujii, T. Onodera, A. Saika, Switching-angle sample-spinning NMR-spectroscopy for obtaining powder-pattern-resolved 2d spectra – measurements of C-13 chemical-shift anisotropies in powdered 3,4-dimethoxybenzaldehyde, Chem. Phys. Lett. 107 (1984) 145–148.
[8] G.E. Maciel, N.M. Szeverenyi, M. Sardashti, Chemical-shift-anisotropy powder patterns by the two-dimensional angle-flipping approach – effects of crystallite packing, J. Magn. Reson. 64 (1985) 365–374.
[9] R.C. Zeigler, R.A. Wind, G.E. Maciel, The stop-and-go spinning technique in MAS experiments, J. Magn. Reson. 79 (1988) 299–306.
[10] L. Frydman, G.C. Chingas, Y.K. Lee, P.J. Grandinetti, M.A. Eastman, G.A. Barrall, A. Pines, Variable-angle correlation spectroscopy in solid-state nuclear-magnetic-resonance, J. Chem. Phys. 97 (1992) 4800–4808.
[11] T. Gullion, Extended chemical-shift modulation, J. Magn. Reson. 85 (1989) 614–619.
[12] R. Tycko, G. Dabbagh, P.A. Mirau, Determination of chemical-shift-anisotropy lineshapes in a two-dimensional magic-angle-spinning NMR experiment, J. Magn. Reson. 85 (1989) 265–274.
[13] M. Carravetta, M. Eden, X. Zhao, A. Brinkmann, M.H. Levitt, Symmetry principles for the design of radiofrequency pulse sequences in the nuclear magnetic resonance of rotating solids, Chem. Phys. Lett. 321 (2000) 205–215.
[14] S.F. Liu, J.D. Mao, K. Schmidt-Rohr, A robust technique for two-dimensional separation of undistorted chemical-shift anisotropy powder patterns in magic-angle-spinning NMR, J. Magn. Reson. 155 (2002) 15–28.
[15] B. Elena, S. Hediger, L. Emsley, Correlation of fast and slow chemical shift spinning sideband patterns under fast magic-angle spinning, J. Magn. Reson. 160 (2003) 40–46.
[16] R. Witter, S. Hesse, U. Sternberg, Powder pattern recoupling at 10 kHz spinning speed applied to cellulose, J. Magn. Reson. 161 (2003) 35–42.
[17] R.M. Orr, M.J. Duer, S.E. Ashbrook, Correlating fast and slow chemical shift spinning sideband patterns in solid-state NMR, J. Magn. Reson. 174 (2005) 301–309.
[18] Y. Nishiyama, T. Yamazaki, T. Terao, Development of modulated rf sequences for decoupling and recoupling of nuclear-spin interactions in sample-spinning solid-state NMR: application to chemical-shift anisotropy determination, J. Chem. Phys. 124 (2006) 064304.
[19] L. Shao, J.J. Titman, Chemical shift anisotropy amplification, Prog. Nucl. Magn. Reson. Spectrosc. 51 (2007) 103–137.
[20] Y. Mou, P.H. Chen, H.W. Lee, J.C.C. Chan, Determination of chemical shift anisotropies of unresolved carbonyl sites by C-alpha detection under magic-angle spinning, J. Magn. Reson. 187 (2007) 352–356.
[21] W.T. Dixon, Spinning-sideband-free NMR-spectra, J. Magn. Reson. 44 (1981) 220–223.
[22] W.T. Dixon, Spinning-sideband-free and spinning-sideband-only NMR-spectra in spinning samples, J. Chem. Phys. 77 (1982) 1800–1809.
[23] A.C. Kolbert, R.G. Griffin, 2-Dimensional resolution of isotropic and anisotropic chemical-shifts in magic angle spinning NMR, Chem. Phys. Lett. 166 (1990) 87–91.
[24] S.F. DeLacroix, J.J. Titman, A. Hagemeyer, H.W. Spiess, Increased resolution in MAS NMR-spectra by 2-dimensional separation of side-band by order, J. Magn. Reson. 97 (1992) 435–443.
[25] O.N. Antzutkin, S.C. Shekar, M.H. Levitt, 2-Dimensional side-band separation in magic-angle-spinning NMR, J. Magn. Reson. Ser. A 115 (1995) 7–19.
[26] D. Massiot, V. Montouillout, F. Fayon, P. Florian, C. Bessada, Order-resolved sideband separation in magic angle spinning NMR of half integer quadrupolar nuclei, Chem. Phys. Lett. 272 (1997) 295–300.
[27] D.J. Aurentz, F.G. Vogt, K.T. Mueller, A.J. Benesi, Multiple-rotor-cycle QPASS pulse sequences: separation of quadrupolar spinning sidebands with an application to La-139 NMR, J. Magn. Reson. 138 (1999) 320–325.
[28] J. Hong, G.S. Harbison, Magic-angle-spinning side-band elimination by temporary interruption of the chemical-shift, J. Magn. Reson. Ser. A 105 (1993) 128–136.
[29] A. Bax, N.M. Szeverenyi, G.E. Maciel, Correlation of isotropic shifts and chemical-shift anisotropies by two-dimensional fourier-transform magic-angle hopping NMR-spectroscopy, J. Magn. Reson. 52 (1983) 147–152.
[30] Z.H. Gan, High-resolution chemical-shift and chemical-shift anisotropy correlation in solids using slow magic angle spinning, J. Am. Chem. Soc. 114 (1992) 8307–8309.
[31] J.Z. Hu, D.W. Alderman, C.H. Ye, R.J. Pugmire, D.M. Grant, An isotropic chemical shift-chemical shift anisotropy magic-angle slow-spinning 2d NMR experiment, J. Magn. Reson. Ser. A 105 (1993) 82–87.
[32] Z.H. Gan, R.R. Ernst, An improved 2D magic-angle-turning pulse sequence for the measurement of chemical-shift anisotropy, J. Magn. Reson. Ser. A 123 (1996) 140–143.
[33] D.W. Alderman, G. McGeorge, J.Z. Hu, R.J. Pugmire, D.M. Grant, A sensitive, high resolution magic angle turning experiment for measuring chemical shift tensor principal values, Mol. Phys. 95 (1998) 1113–1126.
[34] M. Strohmeier, D.M. Grant, A new sensitive isotropic–anisotropic separation experiment – SPEED MAS, J. Magn. Reson. 168 (2004) 296–306.
[35] T. Nakai, D. Kuwahara, Spinning sideband summation for quadrupole MAS NMR spectra using a magic-angle turning technique, Chem. Phys. Lett. 249 (1996) 205–209.
[36] Y.Y. Hu, E.M. Levin, K. Schmidt-Rohr, Broadband "infinite-speed" magic-angle spinning NMR spectroscopy, J. Am. Chem. Soc. 131 (2009) 8390–8391.
[37] O.N. Antzutkin, Sideband manipulation in magic-angle-spinning nuclear magnetic resonance, Prog. Nucl. Magn. Reson. Spectrosc. 35 (1999) 203–266.
[38] M.H. Levitt, P.K. Madhu, C.E. Hughes, Cogwheel phase cycling, J. Magn. Reson. 155 (2002) 300–306.
[39] A. Jerschow, R. Kumar, Calculation of coherence pathway selection and cogwheel cycles, J. Magn. Reson. 160 (2003) 59–64.
[40] B. Henry, P. Tekely, J.J. Delpuech, pH and pK determinations by high-resolution solid-state C-13 NMR: acid–base and tautomeric equilibria of lyophilized L-histidine, J. Am. Chem. Soc. 124 (2002) 2025–2034.